Journal of Cellular Biochemistry 84:68–83 (2002)

Comparative Efficiencies of C-Terminal Signals of Native Glycophosphatidylinositol (GPI)-Anchored Proproteins in Conferring GPI-Anchoring

Rui Chen,[1†] Jansen J. Knez,[1†] William C. Merrick,[2] and M. Edward Medof[1]*

[1]Institute of Pathology, Case Western Reserve University, Cleveland, Ohio, 44106
[2]Department of Biochemistry, Case Western Reserve University, Cleveland, Ohio, 44106

Abstract Every protein fated to receive the glycophosphatidylinositol (GPI) anchor post-translational modification has a C-terminal GPI-anchor attachment signal sequence. This signal peptide varies with respect to length, content, and hydrophobicity. With the exception of predictions based on an upstream amino acid triplet termed ω→ω + 2 which designates the site of GPI uptake, there is no information on how the efficiencies of different native signal sequences compare in the transamidation reaction that catalyzes the substitution of the GPI anchor for the C-terminal peptide. In this study we utilized the placental alkaline phosphatase (PLAP) minigene, miniPLAP, and replaced its native 3′ end-sequence encoding ω-2 to the C-terminus with the corresponding C-terminal sequences of nine other human GPI-anchored proteins. The resulting chimeras then were fed into an in vitro processing microsomal system where the cleavages leading to mature product from the nascent preproprotein could be followed by resolution on an SDS–PAGE system after immunoprecipitation. The results showed that the native signal of each protein differed markedly with respect to transamidation efficiency, with the signals of three proteins out-performing the others in GPI-anchor addition and those of two proteins being poorer substrates for the GPI transamidase. The data additionally indicated that the hierarchical order of efficiency of transamidation did not depend solely on the combination of permissible residues at ω→ω + 2. J. Cell. Biochem. 84: 68–83, 2002.

Key words: GPI anchor; posttranslational processing; native GPI proteins; cell surface engineering

Methodology developed in recent years has made it possible to directly study the sequences that direct transfer of glycosylphosphatidylinositol (GPI) moieties onto proproteins [reviewed in Kodukula et al., 1995]. All known GPI-anchored proteins are synthesized with a C-terminal cleavable peptide [reviewed in Stevens, 1995; Tiede et al., 1999; Sevlever et al., 2000]. The C-terminal peptide (1) is comprised of 15–30 amino acids that are generally hydrophobic, (2) contains no downstream cytosolic domain [Medof and Tykocinski, 1990], and (3) establishes a pattern defined by certain sets of amino acids around the "cleavage-attachment" site [Moran et al., 1991; Gerber et al., 1992]. This site, which is the amino acid left after removal of the C-terminal signal and the attachment of the GPI anchor, has been termed the ω amino acid. Through comparisons of C-terminal polypeptide segments of several GPI-anchored proteins from various species and site-directed mutagenesis of mRNAs, the ω residue for mammalian proteins has been found to be confined to the amino acids G, S, C, A, D, and N [Moran et al., 1991; Gerber et al., 1992].

Analyzing the 15–30 amino acid stretches comprising C-terminal GPI anchor signals with respect to other features which could affect their activities has proven difficult because of the extreme variability of their amino acid sequences. This information is not only relevant for characterization of the GPI transfer

Abbreviations used: GPI, glycophosphatidylinositol; DAF, decay accelerating factor; LFA-3, leukocyte function associated protein-3; CD16, FcγRIII receptor; CD73, 5′ nucleotidase; PLAP, placental alkaline phosphatase; AChE, acetylcholinesterase.

Grant sponsor: NIH; Grant numbers: DK38181, CA81550.

†The first two authors contributed equally to the work.

*Correspondence to: M. Edward Medof, Institute of Pathology, Case Western Reserve University, 2085 Adelbert Road, Cleveland, Ohio 44106.

Received 6 March 2001; Accepted 29 March 2001

DOI 10.1002/jcb.1267

reaction, but is physiologically important both for understanding which proteins will be expressed under conditions in which GPI precursors are limited, e.g., in paroxysmal nocturnal hemoglobinuria (PNH) [Endo et al., 1996], and for artificially modifying conventionally anchored proteins with GPI anchors for purposes of "protein engineering" a.k.a. "painting" of cell surfaces [see Discussion, reviewed in Medof et al., 1996; Hoessli and Robinson, 1998; Fayen et al., 2000].

Studies in the past [Caras, 1991; Moran and Caras, 1991a, b, 1994; Moran et al., 1991; Gerber et al., 1992] that have investigated C-terminal signal features have for the most part done so by employing experimental sequences or by performing site-directed mutagenesis of an individual reporter sequence. These studies in general have found that downstream of $\omega \rightarrow \omega + 2$, any hydrophobic sequence (even an N-terminal sequence or a computer-generated random sequence) will function in the transamidation reaction. In this investigation, we approached the question from a different perspective. We examined signal content as it relates to natural C-terminal sequences evaluating differences in their overall efficiencies in promoting GPI transfer in an effort to gain information relevant to the physiological situation. To ascertain the hierarchy of GPI-anchoring that exists between different native proteins fated to receive GPI anchors (as well as to establish if information encoded in the GPI anchor signal peptide influences protein expression levels on cell surfaces via post-translational control), ten human GPI-anchored proteins; the decay accelerating factor (DAF or CD55), the membrane inhibitor of reactive lysis (CD59), leukocyte function associated protein-3 (LFA-3 or CD58), FcγRIII receptor (CD16), 5′ nucleotidase (CD73), placental alkaline phosphatase (PLAP), acetylcholinesterase (AChE), Thy-1 (CD90), Prion, and CAMPATH (CD52) were chosen for molecular study. Our experimental goal was to define a rank order determining which of these protein's GPI anchor attachment signals is "stronger" than the other resulting in its out-competing the other for GPI anchor addition.

Accordingly, in this study, the cDNA sequences corresponding to the 3′ end signal sequences taken from the above proteins (Table I) were substituted for the native PLAP 3′ end-sequence contained in an engineered form of PLAP cDNA termed miniPLAP. The miniPLAP construct in which PLAP's enzymatic and glycosylation sites [Kodukula et al., 1991] were removed and an M-rich stretch added, was designed to generate a protein smaller than native PLAP so as to allow efficient [^{35}S] monitoring of the C-terminal processing step. After deleting its native GPI-anchor signal, we fused the upstream miniPLAP sequence to the 3′ end signal sequences of each of the listed proteins to generate nine chimeric constructs.

The chimeric cDNAs then were processed in an in vitro microsomal processing system in which four major bands are resolvable after immunoprecipitation on a SDS–PAGE gel system [Kodukula et al., 1991, 1992]. In the case of native miniPLAP, a 28 kDa band (termed "preprominiPLAP") is the primary translation product. A 27 kDa band (termed "prominiPLAP") is the product generated after cleavage of the preprominiPLAP's N-terminal signal sequence by the signal peptidase. A 24.7 kDa band (termed "mature miniPLAP") represents prominiPLAP further processed through concerted removal of the C-terminal GPI anchor signal and concomitant attachment of the GPI anchor moiety. If GPI anchoring fails, a 23 kDa band (termed "free miniPLAP") represents the metabolic dead-end of miniPLAP with its C-terminal GPI signal peptide removed but, as a result of water hydrolysis, OH added to the prominiPLAP ω site.

We approached the question using both conventionally employed and other methods. Five different types of studies were done. In singlet studies, all constructs were run in (1) cotranslational assays and (2) posttranslational assays in which the C-terminal processing step was selectively measured. The constructs were additionally run (3) over a time course allowing analysis of the kinetics of GPI anchor substitution. In "doublet" studies (4 and 5), in vitro and in vivo assays were performed to ascertain how the respective signal sequences competed with each other. To bring out differences in the latter studies, conditions were used in which GPI donors were limited.

MATERIALS AND METHODS

Primers Used in this Study (All 5′ to 3′; F = forward; R = reverse)

DAF F: CCCCCCGCCGGCACCACCTCAGGTACTACCCGTCTTCTA; R: TCTTTGCCAGC-

TABLE I. Native Human C Terminal Signal Sequences

Protein		Signal sequence[a]
PLAP	TD	AAHPGRSVVPALLPLLAGTLLLLETATAP
AChE	HG	EAAPRPGLPLPLLLLHQLLLLFLSHLRRL
CD16	IS	SFSPPGYQVSFCLVMVLLFAVDTGLYFSVKTNI
CD52	PS	ASSNISGGIFLFFVANAIIHLFCFS
DAF	TS	GTTRLLSGHTCFTLTGLLGTLVTMGLLT
CD59	TN	GGTSLSEKTVLLLVTPFLAAAWSLHP
CD73	FS	TGSHCHGSFSLIFLSWAVIFVLYQ
LFA-3	PS	SGHSRHRYALIPIPLAVITTCIVLYMNVL
Prion	GS	SMVLFSSPPVILLISFLIFLIVG
Thy-1	KC	EGISLLAQNTSWLLLLLLSLSLLQATDFMSL

[a]Sequences extending from two amino acids upstream of the cleavage site to the C terminus were used. The space designates the cleavage site.

AGGGTGGCCGCTCGAGCGGCTAAGTCAGC-AAGCCCATGGTTACTAG. Prion F: CCCCC-CGCCGGCACCACCTCGAGCGATGGTCCTC-TTCTCCTC; R: TCTTTGCCAGCAGGGTGG-CCGCTCGAGCGGTCATCATCCCACTATCA-GGAAGATG. Thy-1 F: CCCCCCGCCGGCA-CCACCTGTGAGGGCATCAGCCTG; R: TCT-TTGCCAGCAGGGTGGCCGCTCGAGCGGTC-ACAGGGACATGAAATCCGT. CD16 F: CCC-CCCGCCGGCACCACCTCATCATTCTCTCCA-CCTGGGTACCAAGTC; R: TCTTTGCCAGCA-GGGTGGCCGCTCGAGCGGTCAAATGTTTG-TCTTCACAGAGAA. AChE F: CCCCCCGC-CGGCACCACCCATGGGGAGGCTGCTCCG-AGG; R: TCTTTGCCAGCAGGGTGGCCGCT-CGAGCGGTCACAGCCGCCGGAGGTGGGA. CD52 F: CCCCCCGCCGGCACCACCTCAGC-ATCCAGCAACATAAGC; R: TCTTTGCCAG-CAGGGTGGCCGCTCGAGCGGTCAACTGAA-GCAGAAGAGGTGGAT. CD59 F: CCCCCCG-CCGGCACCACCAATGGTGGGACATCCTTA-TCAGAGAAA; R: TCTTTGCCAGCAGGGT-GGCCGCTCGAGCGGTTAGGGATGAAGGCT-CCAGGCTGC. CD73 F: CCCCCCGCCGGCA-CCACCTCCACAGGAAGTCACTGCCATGGA-AGCTTT; R: TCTTTGCCAATGCATTGGCC-GCTCGAGCGGCTATTGGTATAAAACAAAG-ATCAC. LFA-3 F: CCCCCCGCCGGCACC-ACCAGCAGCGGTCATTCAAGACACAGATA-TGCA; R: TCTTTGCCAGCAGGGTGGCCGCT-CGAGCGGTTAAAGAACATTCTAATACAGC-ACAAT.

Construction of the Various Chimerae

For cartridging in the C-terminal signal sequences of each protein, an *Ngo*MI site proximal to miniPLAP's ω residue [6 nt (2 amino acids) 5′ to the ω cleavage site] and a *Bst*XI site in miniPLAP's 3′ untranslated (UT) region were employed (Fig. 1, panel A). MiniPLAP in the pGEM3Z vector was double-digested. The above described F and R primers containing sequence for upstream *Ngo*MI and downstream *Bst*XI sites were utilized to prime PCR reactions in which the cDNAs of the nine human GPI-anchored proteins were the template DNAs. After cycling for 35 rounds, phenol-extracted PCR products were double-digested with *Ngo*MI and *Bst*XI, purified on 8% polyacrylamide TBE gels, and ligated into the double-cut miniPLAP/pGEM3Z plasmid.

Construction of MiniPLAP cDNA Deletion and Addition Mutants

For the preparation of "microPLAP" cDNA, miniPLAP cDNA in pGEM4Z vector was double-digested with *Eco*52I and *Ngo*MI (Fig. 1, panel B). PCR-amplified sequence starting 123 bp downstream of the *Eco*52I site, prepared with primers containing upstream and downstream *Eco*52I and *Ngo*MI sites, then was cartridged into the double-cut miniPLAP/pGEM4Z construct. For preparing "macroPLAP" cDNA, full-length PLAP cDNA in pGEM4Z was double-digested with *Bgl*II and *Stu*I (Fig. 1, panel C). Upstream and downstream primers containing *Bgl*II and *Stu*I sites were used to amplify 132 bp of in-frame sequence preceding the *Stu*I site in native PLAP cDNA. The doubly-digested PCR product then was ligated into the double-cut miniPLAP/pGEM4Z construct.

Cell Culture, Preparation of K562 Cell Mutants and Isolation of Rough Microsomes (RM)

HeLa cells were grown at 37°C in Dulbecco's minimal essential medium (DMEM) and K562 lines grown in RPMI, both supplemented with 10% newborn calf serum. K562 mutants K and B1 were prepared by N-methyl-N′-nitro-N-

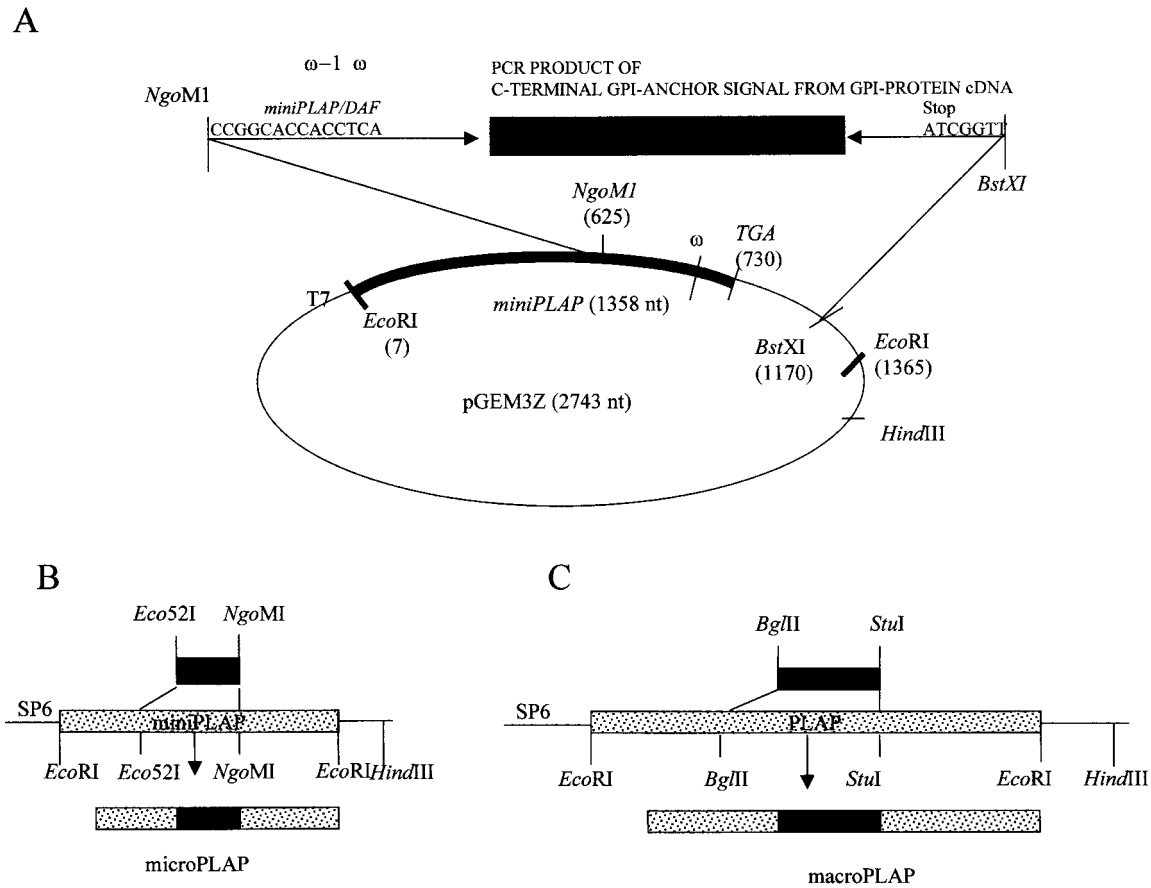

Fig. 1. **A:** Strategy for preparation of chimeric miniPLAP cDNA constructs. The 3′ end-sequence encoding the C-terminal signal peptide of PLAP in pGEM3Z was excised with *Ngo*MI and *Bst*X1. PCR-amplified sequence encoding the C-terminal signals of other native GPI-anchored proteins was prepared with primers containing *Ngo*MI and *Bst*X1 sites, digested with the two enzymes, and cartridged in frame into the correspondingly digested miniPLAP/pGEM3Z construct. **B** and **C:** Strategies used for the preparation of microPLAP and macroPLAP.

nitrosoguanidine (MNNG) mutagenesis followed by GPI-protein negative cell sorting as previously described [Mohney et al., 1994]. Following expansion of the cloned cells, intracellular mannolipid GPI intermediates were characterized by [^{3}H]Mannose (Man) labeling and TLC analyses of butanol partitions of chloroform:methanol:water (10:10:3) extracts [Hirose et al., 1992b]. RM were prepared from cell suspensions by nitrogen cavitation followed by differential centrifugation as previously described [Moran et al., 1991; Chen et al., 1996; Medof et al., 1996].

Co- and Post-translational Processing of mRNAs

Cell-free translation of native and chimeric miniPLAP mRNAs in the presence of rabbit reticulocyte lysate was carried out as described in previous studies [Pelham and Jackson, 1976; Micanovic et al., 1990; Gerber et al., 1992; Chen et al., 1996, 1998; Yu et al., 1997]. Typically, reactions were performed in a 25 μl translation mixture containing 1 μl of 100 ng/μl mRNA, 1.75 μl of [^{35}S]M (15 mCi/ml, 1,100 Ci/mmol, Amersham), 12.5 μl of (nuclease-treated) rabbit reticulocyte lysate, 0.75 μl of a 1 mM amino acid mixture minus M, and 0.5 μl of RNase inhibitor at 40 U/μl (all supplied by Promega Biotec). After addition of 2.5 μl of 100 mM KAc, 4 mM MgAc containing protease inhibitors and 4 μl of RM from a stock containing 50 OD_{280} absorbance units per milliliter, the mixture was incubated at 30°C for the indicated times. Immunoprecipitations were performed with rabbit polyclonal anti-PLAP antibody and protein-A sepharose and eluted products resolved on 15% SDS–PAGE gels. The efficiency of

processing was determined by quantitation of the 24.7 kDa mature miniPLAP band generated by each chimeric construct utilizing autoradiography/densitometry or phosphoimaging and dividing the result by the total density or counts, respectively, in all bands. In replicative experiments, the average difference was ±10% (representative error bars are shown in Figs. 3 and 4).

Preparation of RM Preloaded with Native and Chimeric N-terminal Processed ProminiPLAP

To prepare RM preloaded with the proform of each protein, multiple translation aliquots (25 μl each) containing mRNA were mixed prior to the addition of RM and warmed to 30°C [Maxwell et al., 1995; Ramalingam et al., 1996]. The RM then were added and the mixtures incubated at 30°C for the preloading times (15, 12, or 8 min) specified in each experiment. The samples were placed on ice, pooled and layered over a cushion of 500 mM sucrose, 50 mM TEA. Following centrifugation at 267,000*g* for 15 min at 4°C in a Beckman TLA 100.2 rotor, the supernatant was removed, and the pelleted RM were rinsed with 100 μl of 250 mM sucrose, 50 mM TEA buffer. The preloaded RM then were resuspended in buffer B and 2X energy buffer and the reactions placed back at 30°C for the indicated times.

Kinetic Analyses and Data Calculation

For the kinetic experiments, 12 min preloaded RM were used. The resuspended RM were separated into 12.5 μl aliquots on ice, 12.5 μl of 2X energy buffer added, and the aliquots placed back at 30°C. Reactions were stopped at the indicated times by the addition of SDS destruction buffer and boiling. The kinetic data were analyzed by best fitting the points to a hyperbolic plot using Prism GraphPad. For statistical reasons, at least three time points were used. In general, the goodness of fit (R^2) was 0.95 to 0.99. To compare the relative rates of processing, initial rates were determined from the plots. For those constructs which were processed rapidly (CD73, CD52, and DAF), the values for two (CD52 and DAF) represented minimal estimates since the constructs were more than 50% processed at time zero (see Fig. 5). For the most rapidly processed protein, CD73, it was not possible to estimate the rate as 75% of the protein had been processed at time zero. To better estimate the rate of processing of these latter three signals, shorter processing times were used (6, 9, 12, 15, and 18 min). Under these conditions, better initial rates of processing could be determined for CD52 and DAF while CD73 was still processed past a point at which an accurate initial rate could be determined. As an estimate of the initial rate for CD73, the ratio of the first time point was scaled to that of CD52. Thus the rate of processing of CD73 was estimated to be 1.55 times the initial rate for CD52 ($1.55 \times 2.00 = 3.1$).

Flow Cytometry

Cells (1×10^6) in 25 μl of RPMI were incubated on ice for 15 min with 5 μg/ml of anti-DAF mAB IA10, anti-CD59 mAB 1F5, or respective isotype-matched control. Following washing, resuspension to 25 μl, and secondary incubation on ice for 15 min with 25 μl of 1:50 florescein isothiocyanate (FITC)-labeled sheep anti-mouse Ig (Sigma Chemicals, St. Louis, MO), the washed cells were analyzed on a Becton Dickinson FACScan flow cytometer as described [Chen et al., 1998].

RT-PCR

Pelleted cells (10^6) were lysed in 1 ml of TRIzol reagent (GIBCO BRL). After incubation for 5 min at 20°C, 0.2 ml of chloroform was added, the mixture centrifuged, and RNA precipitated from the supernatant by addition of 0.5 ml of isopropanol. The RNA pellet was washed with 75% ethanol, air dried, and dissolved in water. Total RNA (4 μg) was reverse transcribed using Oligo (dT) 12-18 primer (GIBCO BRL) with 200 U of RNAse H-free reverse transcriptase (Superscript, GIBCO BRL) in a final volume of 20 μl at 42°C for 50 min. The mixtures were sequentially diluted two-fold from 1:8 to 1:128 in water. Two microliter of first strand cDNA was added into a reaction mixture containing 10 μl of 10X PCR buffer (Promega), 10 μl of 25 mM $MgCl_2$, 2 μl each of primer a and b (10 pm/μl each) (5′-TCATGCCCTA-ATCCGGGAGAA-3′ and 5′-TTTTCCTCTGCATTCAGGTGGTG-3′ for DAF; 5′-ATGGGAATCCAAGGAGGG-3′ and 5′-TTAGGGATGAAGGCTCCA-3′ for CD59; and 5′ CCTAGCACCATGAAGATCAA 3′ and 5′ TTTCTGCGCAAGATGGTTTTG-TCAA 3′ for Actin), 2 μl of 10 mM dNTP, 1 μl of Taq DNA polymerase (2–5 U/μl) (Promega) and 71 μl of H_2O. After heating at 94°C for 3 min, amplification was performed by 35 cycles of incubations

for 1 min at 94°C, 1 min at 55°C, and 2 min at 72°C.

RESULTS

Effect of Protein Size on the Efficiency of the GPI Processing Reaction

Because native GPI-anchored proteins differ widely in their sizes, one question relevant to the comparative efficiencies with which they are C-terminally processed is whether polypeptide size affects the GPI anchor substitution reaction. To address this issue, the PLAP C-terminal signal peptide sequence was utilized and the C-terminal processing efficiencies of sequentially smaller PLAP deletion mutants compared to that of full length PLAP (513 amino acids). The results are shown in Figure 2, panel A, with the percent conversion of the proform of each size variant to its GPI-anchored product given below the gels (panel B). As seen, the efficiency of conversion of the four variants (see Fig. 1) ranging in size from the 58 kDa native protein to 15 kDa "microPLAP" varied by less than 10%.

Comparative Processing Efficiencies of Different Native C-Terminal Signals

Preliminary to measurements of the hierarchy of different endogenous C-terminal extension peptides in directing GPI-anchor processing, co-translational assays were performed to verify that each construct was appropriately processed. For these studies, the products obtained using miniPLAP mRNA were compared with those generated using the chimeric miniPLAP mRNAs containing 3′ end-sequences encoding the C-terminal peptides from the nine other proteins studied. Per the standard protocol [Gerber et al., 1992; Chen et al., 1996], the products were analyzed after

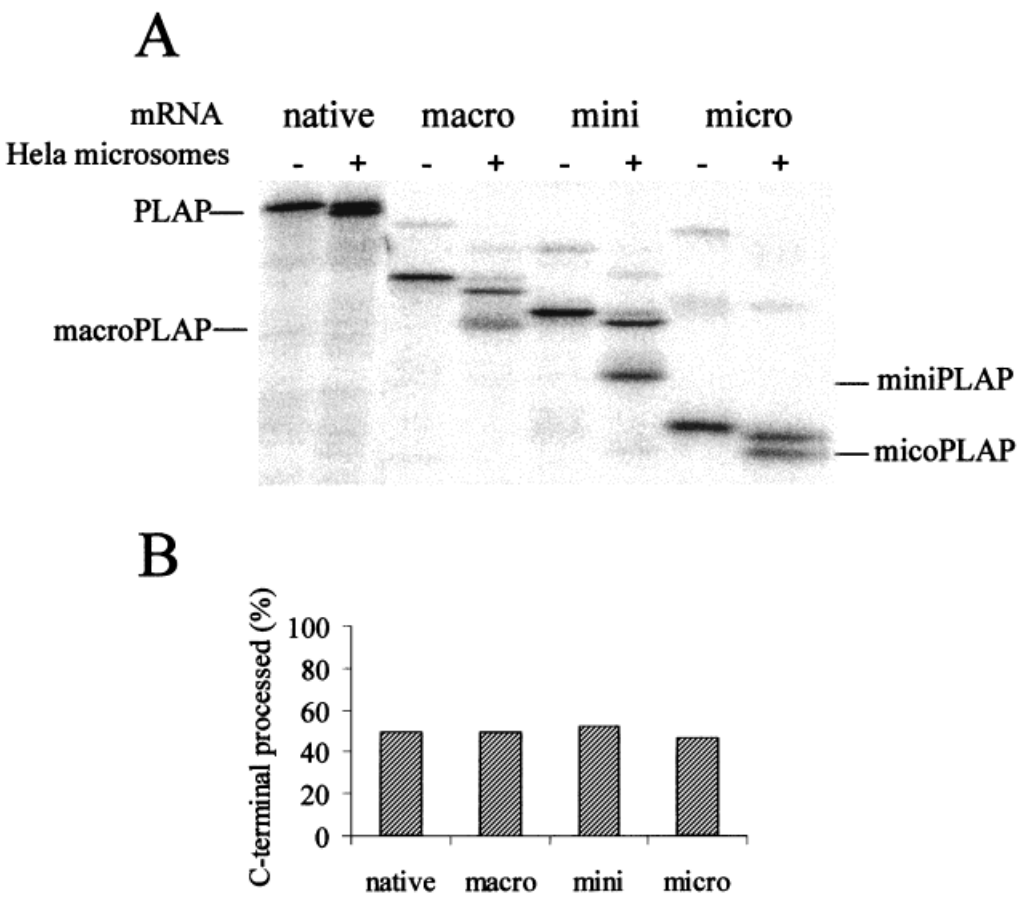

Fig. 2. Effect of polypeptide length on C-terminal processing efficiency. mRNAs encoding intact PLAP, the smaller PLAP protein devoid of PLAP's N-linked glycan (macroPLAP), conventional miniPLAP and the smaller derivative of miniPLAP (microPLAP) were added to HeLa cell RM and the extent of formation of the GPI-anchored product of each protein compared. The experiment was done twice with the same results.

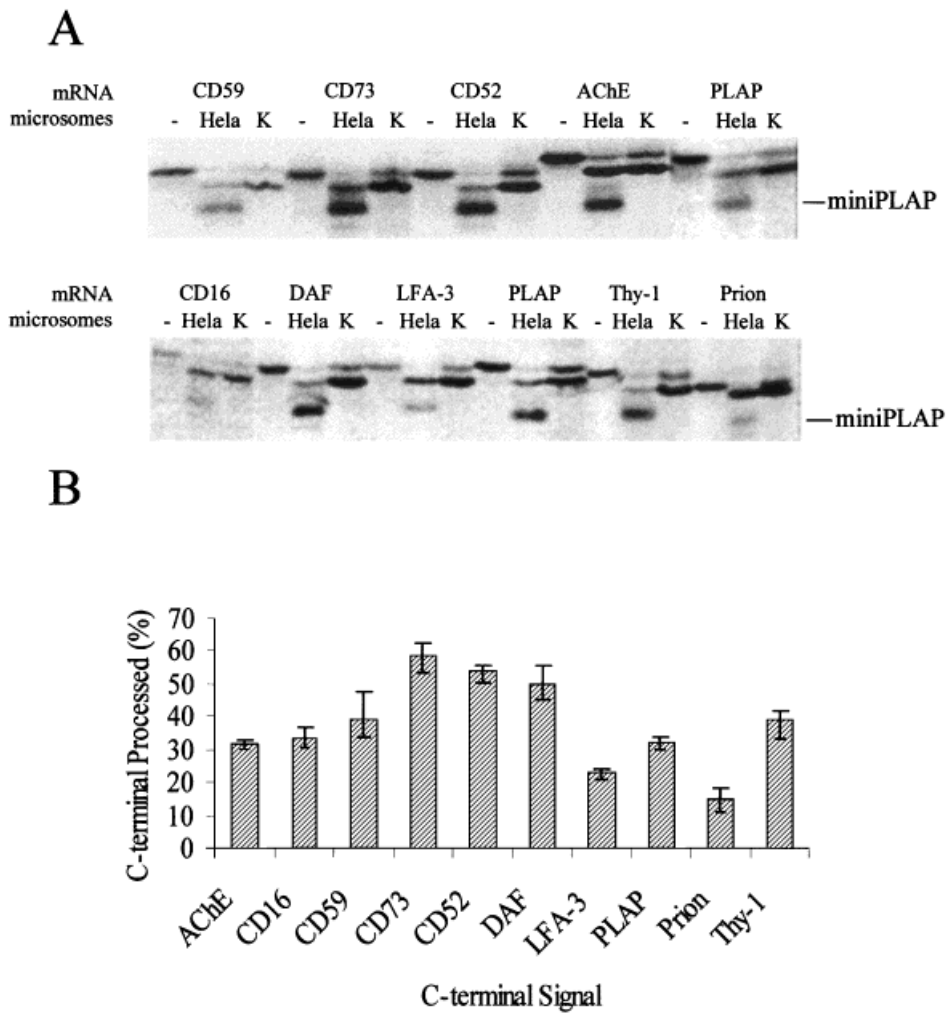

Fig. 3. Comparison of C-terminal signal sequence efficiencies in co-translational assays. mRNAs encoding miniPLAP and each of the chimeric miniPLAP preproproteins (bearing different C-terminal signal sequences) were incubated at 30°C for 90 min with RM from HeLa cells or transamidase-deficient K562 mutant K [Yu et al., 1997] cells. After precipitation with anti-PLAP antibody, the products were analyzed on 15% SDS–PAGE gels. Equivalent results were obtained in two independent experiments.

90 min of incubation. The results are shown in Figure 3. As seen, each construct produced bands consistent with prepro, pro, and GPI-anchored products. The prepro and pro products in each case differed in size due to the varying length of the C-terminal signals (Table I). Control studies with each mRNA using RM from transamidase [GPI8 (see Discussion)) defective K cells [Chen et al., 1996; Yu et al., 1997] verified that the C-terminal processed product in each case was GPI-anchored. As seen from the data, the C-terminal extensions of CD73, CD52, and DAF promoted GPI transfer most efficiently. In contrast, the LFA-3 and Prion extensions were least efficient.

To compare the relative abilities of the different C-terminal peptides to confer GPI anchoring more directly, posttranslational assays next were carried out. For these assays, mRNA was preincubated for 15 min with RM to generate the proform of each protein, and after purifying the RM (see Materials and Methods), the efficiency of the C-terminal processing reaction was subsequently quantified. The experimental read-out thus was independent of translation and of the N-terminal processing step. As shown in Figure 4, with some refinements, a similar hierarchical order of efficiencies of the different signal sequences was observed as seen in Figure 3.

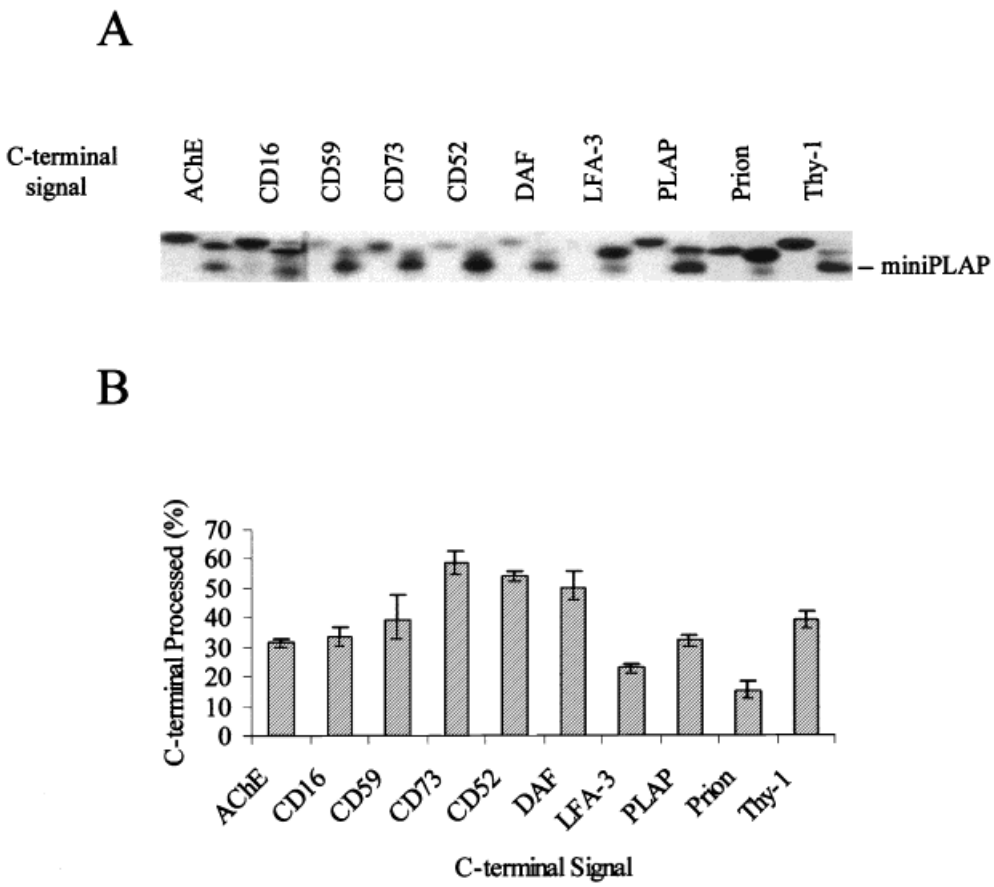

Fig. 4. Comparison of C-terminal signal sequence efficiencies in post-translational assays. mRNAs were incubated with HeLa cell RM as described in the legend of Figure 3, except the reaction was stopped at 15 min. After sedimentation through sucrose cushions, the mixtures were further incubated at 30°C for 75 min. The products were analyzed as in the legend of Figure 3. Equivalent results were obtained in three repeat experiments.

Since the standard posttranslational assay system measures only one time point, i.e., 75 min after the preloaded RM are placed back at 30°C, and processing mediated by different signals could proceed at different rates, kinetic studies next were performed. In these experiments, six constructs were used: native miniPLAP, miniPLAP:CD52, miniPLAP:DAF, miniPLAP:CD73, miniPLAP:CD59, and miniPLAP:AChE. RM were preloaded for 12 rather than 15 min as above (to minimize proprotein processing) and after pelleting through sucrose and transfer back to 30°C, the membranes were harvested at time 0 (after the 12 min preload) and following 10, 20, 40, or 60 min of further incubation. As anticipated (Fig. 5A), the processing of the different signals proceeded at markedly different rates. The CD73 signal was processed so quickly that an initial rate of processing could not be quantitated. Extrapolation of the remaining data to (the projected) time zero and approximation of the initial slopes (see Methods) for the other signals, i.e., PLAP, CD52, DAF, CD59, and AChE, showed that their relative initial processing rates were 0.75, 2.0, 1.2, 1.0, and 0.50%/min, respectively. To better approximate the initial processing rates of the three most efficient signals, i.e., CD73, CD52, and DAF, shorter-term kinetic studies were done (see Methods). These results are shown in Figure 5, panel B. Taking the combined data together, the adjusted overall hierarchical order of efficiency was CD73 (est. 3.1) > CD52 (2.0) > DAF (1.2) > CD59 (1.0) > PLAP (.75) > AChE (.40). In kinetic terms, there was roughly an eight-fold difference in the rate of GPI-anchor addition between the tested sequences. The observed C-terminal

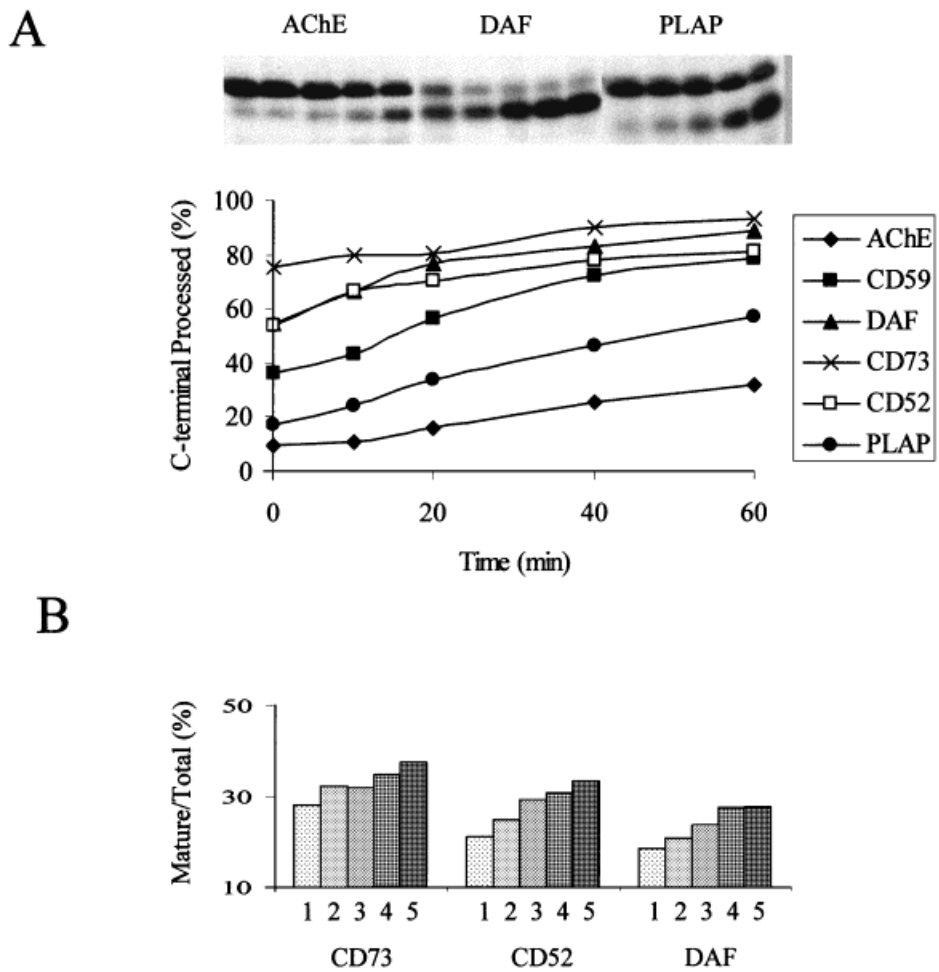

Fig. 5. Comparative kinetics of GPI processing by different C-terminal signal sequences. **A:** mRNAs encoding miniPLAP and 5 chimeric constructs with higher and lower efficiencies based on the results in Figures 3 and 4 were incubated with HeLa cell RM for 12 min at 30°C and the membranes spun through sucrose cushions. The separated, RM containing preloaded preproteins were then placed back at 30°C and samples harvested at 0 min or following 10, 20, 40, or 60 min of further incubation. Products were immunoprecipitated and analyzed as in the legends of Figures 3 and 4. Representative gels (signals slow, fast, and moderate processing efficiencies) are shown above the plot. **B:** Shorter term kinetic studies for the three most efficient signals, i.e., CD73, CD52, and DAF. Lanes 1–5: 6, 9, 12, 15, and 18 min. Because of the short time points of in these studies, cotranslational assays were done as in Figure 3. Equivalent results were obtained in two replicate experiments.

processing efficiencies as determined from the fixed time (75 min) post-translational and kinetic assays are compared in Table I with the theoretical efficiencies as predicted by the permissible $\omega \rightarrow \omega + 2$ combinations [Moran et al., 1991; Stevens, 1995].

Competition Between GPI-anchored Proteins for GPI Donors Under Conditions in Which Donors are Limited

As a final way of assessing the relative capacities of the different signal sequences to promote C-terminal processing, competition assays were set up. Two types of systems were used, the first in vitro and the second in vivo.

In the in vitro assay system, a K562 mutant line with a partial defect in GPI-anchoring was exploited (see Methods). Biosynthetic labeling of the mutant line with [^{3}H]Man showed that it harbored an incomplete block in the addition of the third mannose (Man3) to the glycan core (Fig. 6, panel A). In accordance with the labeling data, standard co-translational processing assays using RM from the mutant line and native miniPLAP mRNA showed that it generated large amounts of hydrolyzed 23 kDa "free

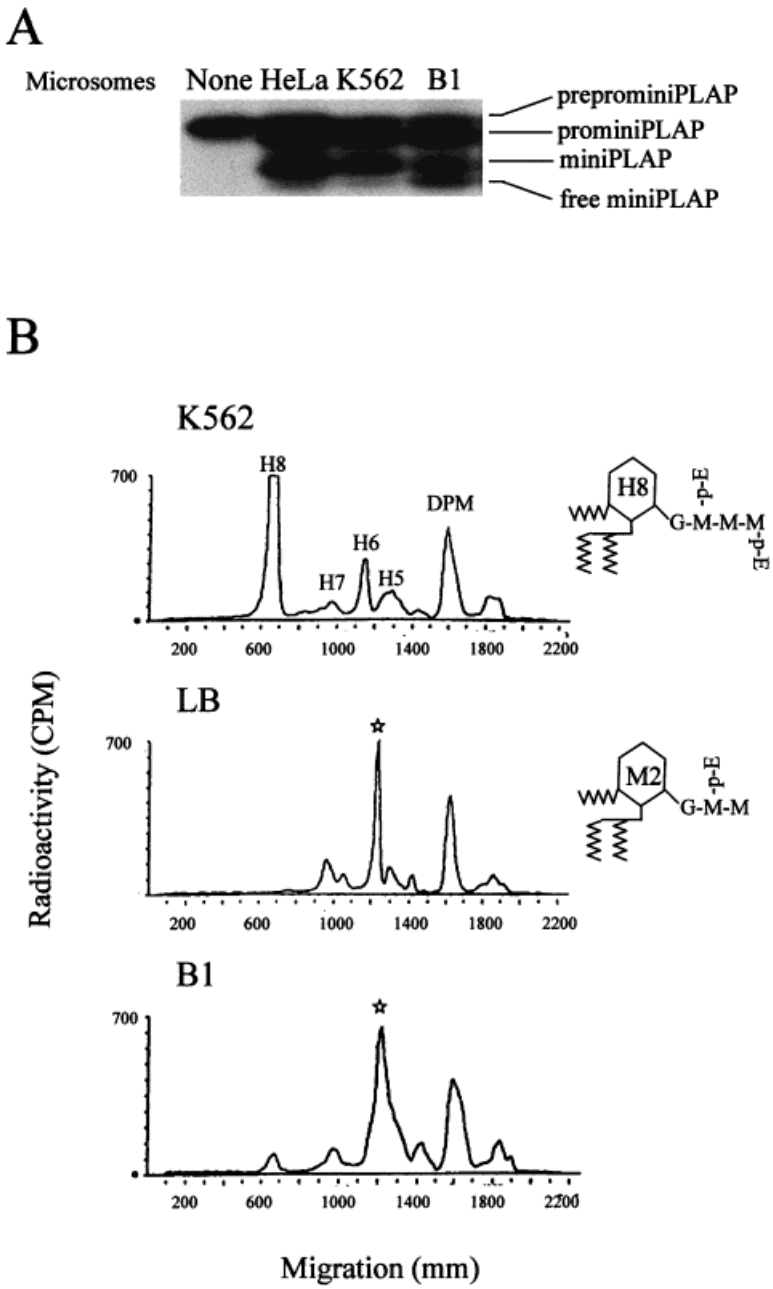

Fig. 6. Biochemical and functional characterization of mutant B1 cells. **A:** Tunicamycin-treated parental K562 cells, mutant B1 cells, and Thy-1-lymphoma class B cells were incubated at 37°C for 2 h with [^{3}H]Man. After extraction with chloroform:methanol:water (10:10:3), mannolipids in butanol partitions were compared by TLC. The B1 mutant accumulated intermediates which comigrated with the respective accumulated products, i.e., Man(EthN-P→)ManGlcN-acyl PI (M2) (shown in the inset) in the Thy-1-class B mutant line [Hirose et al., 1992a]. Only ~10% of fully assembled product, i.e., H8 (also shown in the inset) was found. **B:** miniPLAP mRNA was incubated with RM from Hela cells, parental K562 cells, or B1 mutant cells in cotranslational assays as in Figure 2 the products compared. Large amounts of ''free'' (hydrolyzed) miniPLAP devoid of a GPI anchor was generated by the B1 mutant line.

miniPLAP" (panel B). The mutant was termed B1 (in accordance with the Thy-1 mutant classification scheme). Assays with B1 next were performed as above in single protein experiments. As shown in Figure 7, only three of the signals, CD73, CD52, and DAF (those that were most rapid in the kinetic assays), functioned efficiently.

Next, competition studies were set up. For these experiments, the above-described post-translational system was utilized in which "microPLAP" (see Fig. 2) containing the PLAP C-terminal signal was employed as the source of the competing proprotein. Preliminary kinetic studies showed that the optimal preload time allowing for N-terminal cleavage of the shorter microPLAP preproprotein was 8 min. Based on this result, miniPLAP mRNA or miniPLAP chimeric mRNAs bearing the DAF, or LFA-3 3′ end-sequences mixed with microPLAP mRNA were incubated with B1 RM for 8 min and the RM separated by sedimentation through cold

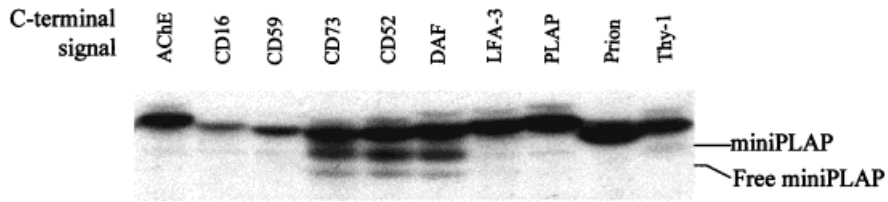

Fig. 7. Comparative efficiencies of C-terminal signals under conditions of limited GPI production. The studies were done as in the legend of Figure 3 except that RM from K562 B1 mutant cells was used. Only the signals of CD73, CD52, and DAF functioned efficiently.

(4°C) sucrose cushions. The preloaded membranes then were placed at 30°C and samples removed after 75 min of incubation. The protein products were precipitated, separated on 17% SDS–PAGE gels, and the production of the GPI-anchored form of each of the proteins compared with that of microPLAP. The results are shown in Figure 8. As seen, (1) the chimeric DAF proprotein was <20% inhibited by microPLAP proprotein in GPI processing, (2) the chimeric LFA-3 proprotein was >60% inhibited in its processing by the concurrent processing of microPLAP proprotein, and (3) standard miniPLAP proprotein functioned with 37% efficiency, a value intermediate between the other two, approximating inhibition by approximately half. Similar results were obtained when the longer preload time (15 min) optimal for miniPLAP was used. The fact that competition was observed between the microPLAP and miniPLAP proproteins is a kinetic confirmation that in the B1 cells, processing is the rate limiting step.

In the second series of experiments conducted in the in vivo state (to test whether the in vitro data can be reflected in cells physiologically), surface DAF and CD59 levels on the B1 K562 cell partial GPI mutant were compared to surface DAF and CD59 levels on parental K562 cells. As shown in Figure 9 panel A, on parental K562 cells, CD59 and DAF florescence levels were 77.5 and 33.2 (corrected mean channel intensities) respectively. In contrast, on the B1 mutant, the florescence levels of the two proteins were 2.2 and 8.0 (corrected mean channel intensities), a greater reduction for CD59 than DAF. Quantitative PCR (Fig. 9, panel B) confirmed that levels of mRNA in the parental and mutant cells were essentially unchanged for DAF and not decreased in the B1 cells for CD59. Although other factors (e.g., rates of protein turnover) can affect steady state surface protein levels, under conditions of limiting GPI donors, the preferential expression of DAF in the B1 K562 cells reflects the same hierarchical order that was observed kinetically (Table II) and directly measured with B1 microsomes themselves in Figure 7, thus, the hierarchical order observed in vitro applies in vivo.

DISCUSSION

According to current concepts, the efficiency of the C-terminal GPI substitution reaction is dependent on the amino acid residues present at the ω to $\omega+2$ consensus site [Moran et al., 1991; Gerber et al., 1992; Ramalingam et al., 1996]. A rank order can be defined among the permissible amino acids at each site that approximates the relative strength of different ω to $\omega+2$ combinations. Several studies [Caras, 1991; Moran and Caras, 1991a, b, 1994; Gerber et al., 1992; Moran et al., 1991] have shown that although the efficiency of the reaction can be influenced by residues in the remainder of the C-terminal signal peptide [Bon et al., 1997; Cross and Boehme, 2000], it does not vary in any as yet apparent systematic way [Udenfriend and Kodukula, 1995]. In this study, we addressed the question concerning the $\omega\rightarrow\omega+2$ consensus and downstream C-terminal signal composition from a different point of view. We focused on native C-terminal signal sequences that are present in the nascent polypeptides of "natural" human GPI-anchored proteins and measured their relative strengths in directing GPI-anchor addition.

For our studies we utilized previously used conventional methods (reviewed in 1) but also employed a number of new approaches. These included kinetic assays, singlet (Fig. 7) and competition studies (Fig. 8) under conditions of limiting donors, and in vivo analyses (Fig. 9). We found that although CD73 was the strongest native GPI addition signal, i.e., in accordance with predictions from the ω to $\omega+2$ residues

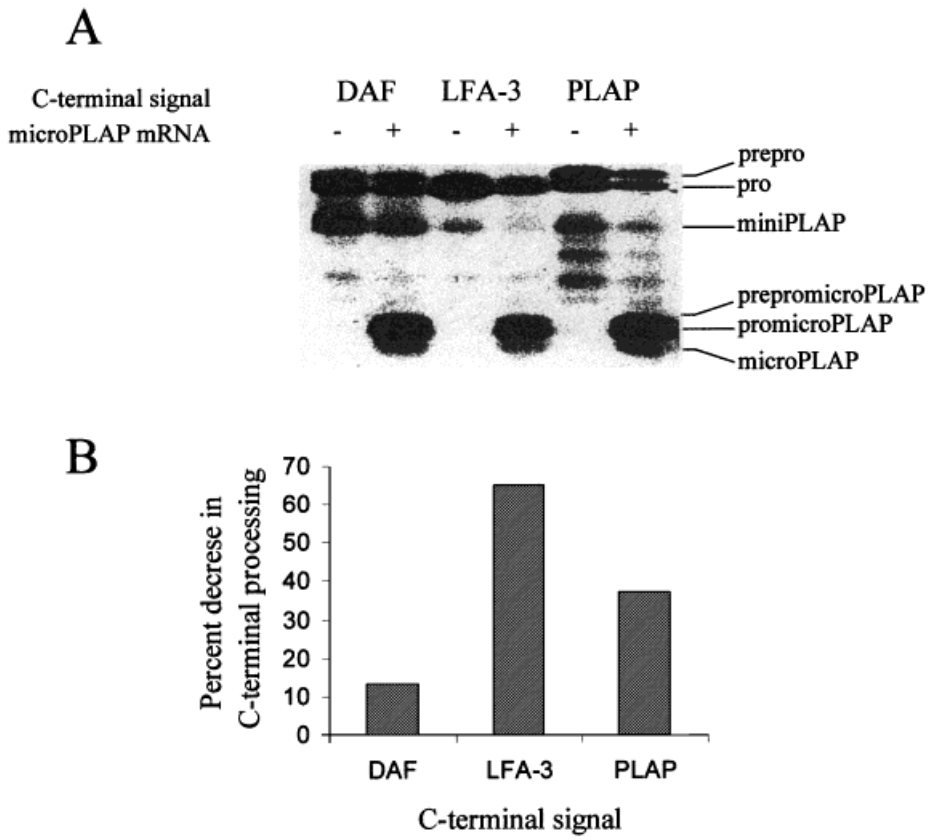

Fig. 8. Competition between different C-terminal signal sequences for GPI anchor substitution. Conventional miniPLAP, the chimeric miniPLAP DAF or the chimeric miniPLAP LFA-3 mRNA mixed with an amount of microPLAP mRNA pre-titered to give equal amounts of product were incubated with half the normal amount of Hela RM in post-translational assays, and the products of each mRNA quantitated. Processing by the DAF signal peptide was $< 20\%$ inhibited, that of the LFA-3 signal was markedly ($> 60\%$) inhibited, and that of the conventional miniPLAP signal 37% reduced (~half-way in between the other two). Densitometry showed that the ratio of label in the competitors in each case was 50, 55, and 45%. The additional bands observed with miniPLAP were not seen in other experiments and are presumably degradation products.

(see Table II), the remainder of the native signals showed significant quantitative differences and defined a different rank order. For example, using the standard preload data, whereas the ω to $\omega+2$ predictions for LFA-3 and Thy-1 were > 80 and $< 54\%$ of that of CD73, respectively, the relative efficiencies of the two signals experimentally were found to be 23 and 80% of that of CD73. The kinetic data brought out bigger differences, e.g., whereas the ω to $\omega+2$ predictions for PLAP were $> 80\%$ of that of CD73, its relative efficiency experimentally was found to be only 24% of that of CD73.

One issue that has not been explored in the past is whether the size of the N-terminally processed proprotein affects the efficiency of the C-terminal processing reaction. It is not known how the proprotein reacts with the transamidase machinery. BIP is involved in the overall reaction but is thought to participate prior to the transamidation in which the GPI moiety is substituted for the C-terminal signal [Amthauer et al., 1992; Vidugiriene and Menon, 1995; Oda et al., 1996]. In the case of N-glycosylation, this issue has not been studied, but the position of the NXS consensus relative to other sequence elements and the extent of folding have been found to be critical determinants [Liebhaber et al., 1992; Shakin-Eshleman et al., 1992, 1993; Shakin-Eshleman, 1996]. Our data using progressively smaller PLAP deletion mutants indicate that the size of the proprotein per se is not an important determinant. In view of structural studies that full-length PLAP is glycosylated [Watanabe et al., 1992] and disulfide-bonded, and has a unique conformation definable by mABs [Hoylaerts and Millan, 1991], the data also argue that to the extent it

TABLE II. Relative GPI-Anchoring Efficiencies of Native C-Terminal Signal Sequences

Signal peptide	ω	ω + 1	ω + 2	Predicted[a] (×)	Predicted[b] (+)	Preload[c]	Kinetics[d]
CD73	S (1)	T (0.7)	G (0.7)	1.0	1.0	1.0	1.0
CD52	S (1)	A (1)	S (0.3)	0.61	0.96	0.97	0.65
DAF	S (1)	G (+)	T (0.1)	$0.02 < x < 0.20$	$0.46 < x < 0.86$	0.93	0.39
CD59	N (0.8)	G (+)	G (0.7)	$0.11 < x < 1.14$	$0.63 < x < 1.04$	0.83	0.32
Thy-1	C (0.2)	E (0.4)	G (0.7)	0.11	0.54	0.80	
PLAP	D (0.4)	A (1)	A (1)	0.82	1.0	0.72	0.24
CD16	S (1)	S (0.6)	F (N/A)	$0.12 < x < 1.22$	$0.67 < x < 1.1$	0.48	
AChE	G (0.4)	E (0.4)	A (1)	0.33	0.75	0.43	0.13
LFA-3	S (1)	S (0.6)	G (0.7)	0.86	0.96	0.23	
Prion	S (1)	M(0.3)	V (0.1)	0.06	0.58	0.16	

N/A = not done; + = functional but not quantitated.
[a]The predicted efficiency was calculated by multiplying the values at the ω, ω + 1 and ω + 2 sites [Gerber et al., 1992] and normalizing them relative to the most efficient combination.
[b]Predicted efficiency calculated by adding the values at the ω, ω + 1 and ω + 2 sites [Gerber et al., 1992] and normalizing them as in [a].
[c]Data from Figure 4.
[d]Data from Figure 5.

is folded, the folding at sites distant from the C-terminus also is not an important determinant.

Our initially performed cotranslational assays (Fig. 3) were able to distinguish between the stronger (CD73, CD52, DAF, and Thy-1) and weaker (AChE, LFA-3, and Prion) signal sequences. That the differences in fact reflected differences in the C-terminal processing reaction was verified by our posttranslational assays (Fig. 4). The full extent of the differences between the various signals did not become evident, however, until the reactions were assessed kinetically (Fig. 5). These latter studies showed a ~8-fold range of efficiencies for the six different native signal peptides studied (likely a much greater range for the ten signal peptides used in the overall study since there was a >6-fold range in the less sensitive conventional posttranslational studies).

The results of our study may provide information relevant to the biochemical requirements which underlie how the GPI transfer machinery functions. Other work [Hamburger et al., 1995; Ohishi et al., 1995; Benghezal et al., 1996; Yu et al., 1997; Hiroi et al., 1998] has shown that the "transamidase" complex which mediates the reaction contains the two components, Gpi8p and Gaa1p. It is likely that additional elements are involved (as in the six component N-terminal signal peptidase). Gpi8p is a 348 amino acid long type I ER protein with a short C-terminal cytoplasmic sequence and large lumenally oriented N-terminal domain [Benghezal et al., 1996]. Its N-terminal domain contains a segment which shows homology to a family of plant transamidases and according to currently available data (see below), contains the enzymatic site. Mutagenesis of the predicted active S-residue abolishes its function [Ohishi et al., 2000]. Human Gaa1p is a 621 amino acid long ER protein with 7 membrane spanning domains at its C-terminus, and a large 306 amino acid long lumenal domain [Hamburger et al., 1995; Hiroi et al., 2000]. Studies utilizing chimeric Gaa1p proteins in which the yeast and human sequences for the 306 amino acid long intraluminal domain were interchanged [Ohishi et al., 1998] have provided indirect evidence that this portion of Gaa1p recognizes the ω to ω + 2 consensus on the nascent proprotein. Recent in vitro studies [Chen and Medof, 2000], in which miniPLAP mRNA was translated in the presence of Gpi8p- and Gaa1p-deficient microsomes preloaded with [^{35}S]Gpi8p or [^{35}S]Gaa1p and anti-PLAP immunoprecipitates analyzed, have provided evidence that the proprotein interacts with Gaa1p in the Gaa1p/Gpi8p complex. The studies additionally have shown that Gpi8p forms a covalent intermediate with the proprotein (Chen R, Hiroi Y, Anderson V, and Medof E, unpublished observations). Our findings that C-terminal processing efficiency is not readily predicted from ω to ω + 2 combinations alone, argues that interaction of the proprotein with transamidase elements is influenced by additional amino acids or, possibly, that its prior interaction with the translocon plays an indirect role in the efficiency of its presentation to or processing by the transamidation machinery.

The hierarchical order of GPI processing efficiencies of different native C-terminal signal sequences defined in this study in principle has relevance clinically. In some patients with the

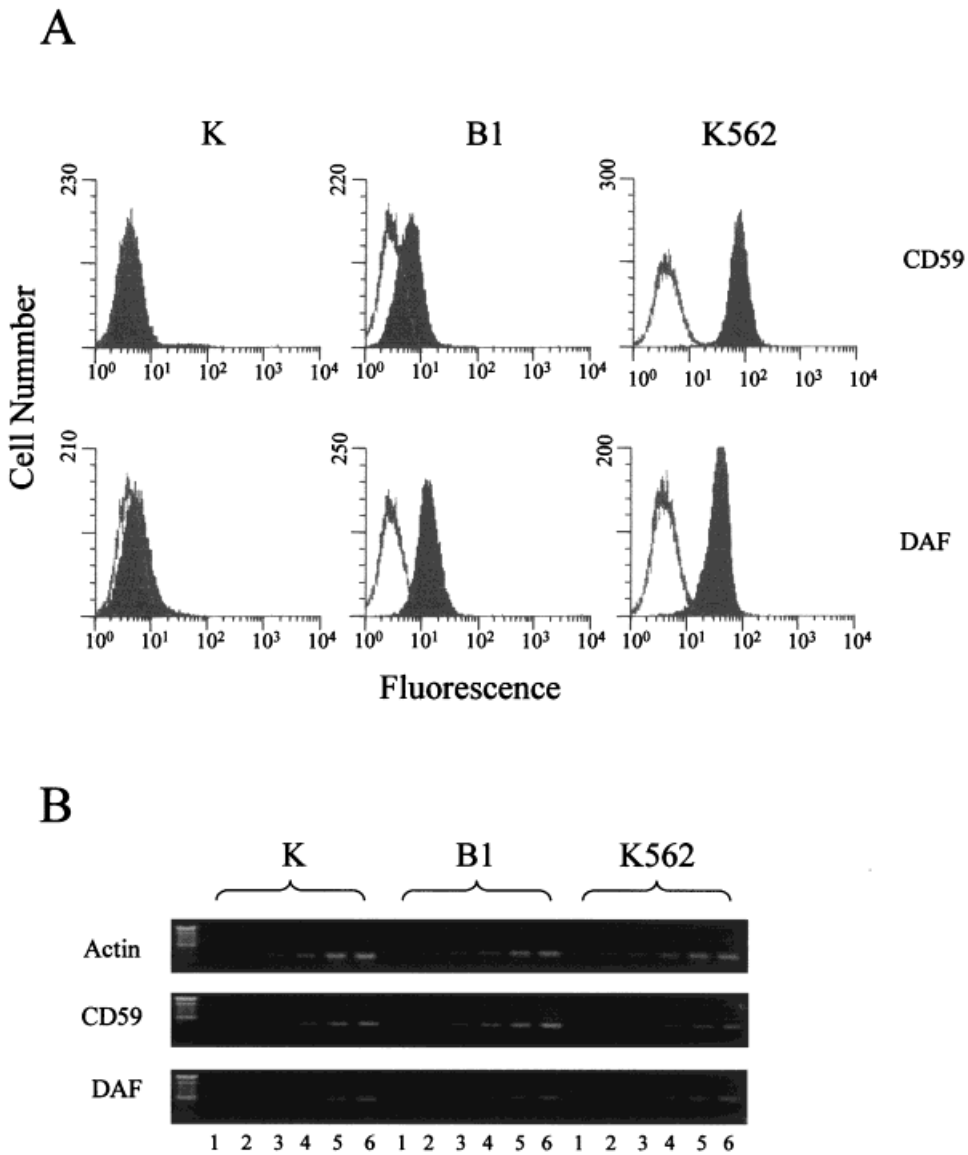

Fig. 9. **A:** Flow cytometric analyses of parental K562 and B1 and K mutant cells. The cells were stained in an identical fashion with the same anti-DAF and anti-CD59 mABs as described in the Methods [Chen et al., 1998]. KA = K562 cells; K = K562 mutant cells deficient in the GPI8 transamidase; B1 = K562 mutant cells [termed M2 (Fig. 6)] with a partial block in the addition of Man3 to the glycan core (see Text). **B:** Semiquantitative PCR of CD59, DAF, and actin mRNAs in parental K562 cells and the two mutant lines.

acquired hemolytic disorder PNH, mutation of the affected gene termed PIG-A eventuates in a partial rather than a complete defect in GPI-anchoring [Norris et al., 1997]. Mutated cells of these patients exhibit some but not other GPI-anchored surface proteins. Although in accordance with our data preferential expression of DAF vs. CD59 [Endo et al., 1996] has been described, a comprehensive study of different GPI-anchored proteins on different blood cell types, e.g., CD73, CD52, DAF, CD59, and LFA-3 on affected lymphocytes, in this situation has not been carried out.

Finally, the data obtained in this study are important for the newly developing technology of "protein engineering" or cell surface "painting" [Medof et al., 1996; Tykocinski et al., 1996; Hoessli and Robinson, 1998; Fayen et al., 2000]. In this technique, a chimeric cDNA is generated in which the C-terminal signal sequence of a GPI-anchored protein is substituted for the endogenous C-terminal sequence of the protein

chosen for study (either transmembrane or soluble), the chimeric cDNA is expressed in a suitable cell line, and the GPI-anchored product is purified. The purified GPI protein then is incubated with the target cell of interest resulting in its stable and physiologically correct incorporation into that cell's lipid bilayer. This technique allows any protein to be transferred to any cell and thus provides an alternative to gene transfer that has practical advantages [reviewed in Medof et al., 1996; Tykocinski et al., 1996]. This methodology has been exploited in the past for a wide range of proteins. For these studies several different native C-terminal signal sequences have been used arbitrarily [Medof et al., 1996]. In principle, ultimately it may be possible to specifically engineer a higher efficiency C-terminal signal. In the meantime, by selecting C-terminal signal sequences based on their relative efficiencies as described above, the findings in this study should allow for further optimization of one important element of this methodology.

ACKNOWLEDGMENTS

The authors thank Dr. Sidney Udenfriend (Drew University, Madison, NJ) for reagents and helpful discussion, Dr. Vernon Anderson (Case Western Reserve University, Cleveland, OH) for critical reading, and Sara Cechner for manuscript preparation.

REFERENCES

Amthauer R, Kodukula K, Brink L, Udenfriend S. 1992. Phosphatidylinositol-glycan (PI-G)- anchored membrane proteins: requirement of ATP and GTP for translation-independent COOH-terminal processing. Proc Natl Acad Sci USA 89:6124–6128.

Benghezal M, Benachour A, Rusconi S, Aebi M, Conzelmann A. 1996. Yeast Gpi8p is essential for GPI anchor attachment onto proteins. EMBO J 15:6575–6583.

Bon S, Coussen Fj, Massoulie J. 1997. Sequence requirements of the GPI cleavage/addition site in rat acetylcholinesterase: "the Interaction of GPI Anchors with Biological Membranes.": Splugen, Switzerland.

Caras IW. 1991. Probing the signal for glycophosphatidylinositol anchor attachment using decay accelerating factor as a model system. Cell Biol Int Rep 15: 815–826.

Chen R, Medof ME. 2000. Nascent proproteins interact with Gaalp independently of Gpi8p and of the ω site residues " the 2000 FASEB Summer Research Conference, Lipid Modifications of Proteins." Copper Mountain, Colorado, USA.

Chen R, Udenfriend S, Prince GM, Maxwell SE, Ramalingam S, Gerber LD, Knez J, Medof ME. 1996. A defect in glycophosphatidylinositol (GPI) surface proteins. Proc Natl Acad Sci USA 93:2280–2284.

Chen R, Walter EI, Parker G, Lapuraga JP, Millan JL, Ikehara Y, Udenfriend S, Medof ME. 1998. Mammalian glycophosphatidylinositol anchor transfer to proteins and posttransfer deacylation. Proc Natl Acad Sci USA 95:9512–9517.

Cross GAM, Boehme U. 2000. Mutational analysis of the variant surface glycoprotein GPI-anchor signal sequence in *Trypanosoma brucei* "the FASEB Summer Research Conference, "Lipid Modifications of Proteins"." Copper Mountain, Colorado.

Endo M, Ware RE, Vreeke TM, Singh SP, Howard TA, Tomita A, Holguin MH, Parker CJ. 1996. Molecular basis of the heterogeneity of expression of glycosyl phosphatidylinositol anchored proteins in paroxysmal nocturnal hemoglobinuria. Blood 87:2546–2557.

Fayen JD, Tykocinski ML, Medof ME. 2000. Glycerolphosphoinositide anchors for membrane-tethering proteins. Methods Enzymol 327:351–368.

Gerber LD, Kodukula K, Udenfriend S. 1992. Phosphatidylinositol glycan (PI-G) anchored membrane proteins: amino acid requirements adjacent to the site of cleavage, and PI-G attachment in the COOH-terminal signal peptide. J Biol Chem 267:12168–12173.

Hamburger D, Egerton M, Riezman H. 1995. Yeast Gaalp is required for attachment of a completed GPI anchor onto proteins. J Cell Biol 129:629–639.

Hiroi Y, Komuro I, Chen R, Hosoda T, Mizuno T, Kudoh S, Georgescu SP, Medof ME, Yazaki Y. 1998. Molecular cloning of human homolog of yeast GAA1 which is required for attachment of glycophosphatidylinositols to proproteins. FEBS Lett 421:252–258.

Hiroi Y, Chen Rj, Sawa H, Hosoda T, Kudoh Sj, Kobayashi Y, Aburatani H, Nagashima K, Nagai R, Yazaki Y, Medof ME, Komuro I. 2000. Cloning of murine glycosyl phosphatidylinositol anchor attachment protein, GPAAl. Am J Physiol Cell Physiol 279:C205–C212.

Hirose S, Prince GM, Sevlever D, Ravi L, Rosenberry TL, Ueda E, Medof ME. 1992a. Characterization of putative glycoinositol phospholipid anchor precursors in mammalian cells. Localization of phosphoethanolamine. J Biol Chem 267:16968–16974.

Hirose S, Ravi L, Prince GM, Rosenfeld MG, Silber R, Andresen SW, Hazra SV, Medof ME. 1992b. Synthesis of mannosylglucosaminylinositol phospholipids in normal but not paroxysmal nocturnal hemoglobinuria cells. Proc Natl Acad Sci USA 89:6025–6029.

Hoessli DC, Robinson PJ. 1998. GPI-anchors and cell membrances: a special relationship. Trends Cell Biol 8:87–89.

Hoylaerts MF, Millan JL. 1991. Site-directed mutagenesis and epitope-mapped monoclonal antibodies define a catalytically important conformational difference between human placental and germ cell alkaline phosphatase. Eur J Biochem 202:605–616.

Kodukula K, Micanovic R, Gerber L, Tamburrini M, Brink L, Udenfriend S. 1991. Biosynthesis of phosphatidylinositol glycan-anchored membrane proteins. Design of a simple protein substrated to characterize the enzyme that cleaves the COOH-terminal signal peptide. J Biol Chem 266:4464–4470.

Kodukula K, Cines D, Amthauer R, Gerber L, Udenfriend S. 1992. Biosynthesis of phosphatidylinositol-glycan(PI-G)-

anchored membrane proteins in cell-free systems: cleavage of the nascent protein and addition of the PI-G moiety depend on the sixe of the COOH-terminal signal peptide. Proc Natl Acad Sci USA 89:1350–1353.

Kodukula K, Maxwell SE, Udenfriend S. 1995. Processing of nascent proteins to glycosylphosphatidylinositol-anchored forms in cell-free systems. Methods Enzymol 250:536–547.

Liebhaber SA, Cash F, Eshleman SS. 1992. Translation inhibition by an mRNA coding region secondary structure is determined by its proximity to the AUG initiation codon. J Mol Biol 226:609–621.

Maxwell SE, Ramalingam S, Gerber LD, Udenfriend S. 1995. Cleavage without anchor addition accompanies the processing of a nascent protein to its glycosylphosphatidylinositol-anchored form. Proc Natl Acad Sci USA 92: 1550–1554.

Medof ME, Tykocinski ML. 1990. The cytoplasmic extension as a determinant for glycoinositolphospholipid anchor substitution. In: Welply JK, Jaworski E, editors. "Glycobiology." New York: Wiley-Liss. p 17–22.

Medof ME, Nagarajan S, Tykocinski ML. 1996. Cell surface engineering with GPI- anchored proteins. FASEB J 10:574–586.

Micanovic R, Kodukula K, Gerber LD, Udenfriend S. 1990. Selectivity at the cleavage/attachment site of phosphatidylinositol-glycan anchored membrane proteins is enzymatically determined. Proc Natl Acad Sci USA 87: 7939–7943.

Mohney RP, Knez JJ, Ravi L, Sevlever D, Rosenberry TL, Hirose S, Medof ME. 1994. Glycoinositol phospholipid anchor defective K562 mutants with biochemical lesions distinct from those in Thy-1-negative murine lymphoma mutants. J Biol Chem 269:6536–6542.

Moran P, Caras IW. 1991a. Fusion of sequence elements from non-anchored proteins to generate a fully functional signal for glycophosphatidylinositol membrane anchor attachment. J Cell Biol 115:1595–1600.

Moran P, Caras IW. 1991b. A nonfunctional sequence converted to a signal for glycophosphatidylinositol membrane anchor attachment. J Cell Biol 115:329–336.

Moran P, Caras IW. 1994. Requirements for glycosylphosphatidylinositol attachment are similar but not identical in mammalian cells and parasitic protozoa. J Cell Biol 125:333–343.

Moran P, Raab H, Kohr WJ, Caras IW. 1991. Glycophospholipid membrane anchor attachment. Molecular analysis of the cleavage/attachment site. J Biol Chem 266:1250–1257.

Norris ER, Howard TA, Marcus SJ, Ware RE. 1997. Structural and functional analysis of the Pig- a protein that is mutated in paroxysmal nocturnal hemoglobinuria. Blood Cells Mol Dis 23:350–360.

Oda K, Wada I, Takami N, Fujiwara T, Y M, Ikehara Y. 1996. BiP/GRP78 but not calnexin associates with a precursor of GPI-anchored protein. Biochem J 316:623–630.

Ohishi K, Inoue N, Endo Y, Fujita T, Takeda J, Kinoshita T. 1995. Structure and chromosomal localization of the GPI-anchor synthesis gene PIGF and its pseudogene *PIGF. Genomics 29:804–807.

Ohishi K, Inoue N, Takeda J, Hamburger D, Riezman H, Kinoshita T. 1998. GAA1 recognizes the GPI anchor attachment signals and is complexed with GPI8 to form a GPI transamidase. Mol Immunol 35:388. (abstr).

Ohishi K, Inoue N, Maeda Y, Takeda J, Riezman H, Kinoshita T. 2000. Gaa1p and Gpi8p are components of a glycosylphosphatidylinositol (GPI) transamidase that mediates attachment of GPI to proteins. Mol Biol Cell 11:1523–1533.

Pelham HR, Jackson RJ. 1976. An efficient mRNA-dependent translation system from reticulocyte lysates. Eur J Biochem 67:247–256.

Ramalingam S, Maxwell SE, Medof ME, Chen R, Gerber LD, Udenfriend S. 1996. COOH-terminal processing of nascent polypeptides by the glycosylphosphatidylinositol transamidase in the presence of hydrazine is governed by the same parameters as glycosylphosphatidylinositol addition. Proc Natl Acad Sci USA 93:7528–7533.

Sevlever D, Chen R, Medof ME. 2000. Synthesis of the GPI anchor. In: Young NS, Moss J, editors. Paroxysmal Nocturnal Hemoglobinuria and the Glycophosphoinositol-Linked Proteins.". San Diego: CA: Academic Press. p 199–220.

Shakin-Eshleman SH. 1996. Regulation of site-specific N-linked glycosylation. Trends Glycosci Glycotechnol 267:10690–10698.

Shakin-Eshleman SH, Remaley AT, Eshleman JR, Wunner WH, Spitalnik SL. 1992. N-linked glycosylation of rabies virus glycoprotein. Individual sequons differ in their glycosylation efficiencies and influence on cell surface expression. J Biol Chem 267:10690–10698.

Shakin-Eshleman SH, Wunner WH, Spitalnik SL. 1993. Efficiency of N-linked core glycosylation at asparagine-319 of rabies virus glycoprotein is altered by deletions C-terminal to the glycosylation sequon. Biochemistry 32: 9465–9472.

Stevens VL. 1995. Biosynthesis of glycosylphosphatidylinositol membrane anchors. Biochem J 310:361–370.

Tiede A, Bastisch I, Schubert J, Orlean P, Schmidt RE. 1999. Biosynthesis of glycosylphosphatidylinositols in mammals and unicellular microbes. Biol Chem 380:503–523.

Tykocinski ML, Kaplan DR, Medof ME. 1996. Antigen-presenting cell engineering. The molecular toolbox. Am J Pathol 148:1–16.

Udenfriend S, Kodukula K. 1995. Prediction of omega site in nascent precursor of glycosylphosphatidylinositol protein. Methods Enzymol 250:571–582.

Vidugiriene J, Menon AK. 1995. Soluble constituents of the ER lumen are required for GPI anchoring of a model protein. EMBO J 14:4686–4694.

Watanabe T, Wada N, Chou JY. 1992. Structural and functional analysis of human germ cell alkaline phosphatase by site-specific mutagenesis. Biochemistry 31: 3051–3058.

Yu J, Nagarajan S, Knez JJ, Udenfriend S, Chen R, Medof ME. 1997. The affected gene underlying the class K surface protein defects. Codes for the GPI-transamidase. Proc Natl Acad Sci USA 94:12580–12585.